Multi-objective Crashworthiness Optimization of the Aluminum Foam-filled Tubes

A. Khalkhali[1]*, S. Samareh Mousavi [2]

[1] Assistant professor, [2] BSc. Student, School of Automotive Engineering, Iran University of Science and Technology, Tehran, Iran

* Corresponding Author

Abstract

In order to reduce both the weight of vehicles and the damage of occupants in a crash event simultaneously, it is necessary to perform a multi-objective optimization of the automotive energy absorbing components. In this paper, axial impact crushing behavior of the aluminum foam-filled thin-walled tubes are studied by the finite element method using commercial software ABAQUS. Comparison of the present simulation results with the results of the experiments reported in the previous works indicated the validity of the numerical analyses. A meta-model based on the feed-forward artificial neural networks are then obtained for modeling of both the absorbed energy (E) and the peak crushing force (Fmax) with respect to design variables using those data obtained from the finite element modeling. Using such obtained neural network models, a modified multi-objective GA is used for the Pareto-based optimization of the aluminum foam-filled thin-walled tubes considering three conflicting objectives such as energy absorption, weight of structure, and peak crushing force.

Keywords: Aluminum foam, Crashworthiness, MLF, Multi-objective optimization, Genetic Algorithm, Pareto.

1. INTRODUCTION

Advances in technology have led to higher speed of transportation which increases the probability of traffic accident and serious human damages. Design of auxiliary metal structural components capable to sustain prescribed loads and dissipate undesirable energies while undergoing plastic deformation is one of the prime means of energy release protection. Therefore, the crash characteristics of energy absorbing components have received considerable attention over the past decades [1-5].

In recent years, researchers have shown an interest in using cellular structures (honeycombs, foams, etc.) for energy absorption devices. Foams due to their low weight and good crushing behaviors are nearly ideal energy absorbers [6-8]. Using of aluminum foam because of its efficiency and reproducible production routes have been developed in the last year [9]. Nowadays, the design of modern vehicle structure is driven by many competing criteria. Vehicle weight reduction has been prevalent in the automotive industry to reduce the fuel consumption. On the other hand, design of structural components for the purpose of both absorbing kinetic energy and attenuating the maximum crushing force have become a special topic in design research to ensure the occupant safety in the event of a crash. Therefore, the energy absorbing capability, the weight of energy absorbing components, and the maximum crushing load are important objective functions to be optimized simultaneously as a complex multi-objective optimization problem (MOP). In order to trade-off among these conflicting objectives, the Pareto based approach is considered in this work for such MOP. It has been shown by some of authors [10] that very interesting and important design facts can be discovered by the Pareto-based optimization of energy absorption systems. However, considering the computational cost of performing such multi-objective optimization of a complete dynamic model , the direct use of FEM software is prohibitive, if not impossible. Therefore, it would be greatly desirable to use alternate simplified models instead of time-consuming FEM during optimization process. In this

way, either finite element analysis or experimental procedure may be performed to obtain some training and testing data for developing that meta-model.

In fact, system identification and modeling of complex processes using input-output data have always attracted many research efforts. In fact, system identification techniques are applied in many fields in order to model and predict the behaviors of unknown and/or very complex systems based on given input-output data [11]. In this way, soft-computing methods [12], which concern computation in an imprecise environment, have gained significant attention. The main components of soft computing, namely, fuzzy logic, neural network, and evolutionary algorithms have shown great ability in solving complex non-linear system identification and control problems. Many research efforts have been expended to use of evolutionary methods as effective tools for system identification [13-18]. Among these methodologies, multi-layer feed-forward (MLF) artificial neural networks with a single hidden sigmoid layer and biases are the most frequently used networks because of their ability to approximate any function with a finite number of discontinuities [19-21].

The present study aims at maximizing the energy absorption capacity (E), minimizing the weight of energy absorption structure (W), and minimizing the peak crushing force (Fmax) for aluminum foam-filled thin-walled tubes. Finite element modeling (FEM) using commercial software ABAQUS are first employed to determine the effects of geometrical design variables on the energy

absorption and peak crushing force. A multi-layered feed-forward neural network is then constructed to precisely establish the relationship

between those objective functions (E and Fmax) and the design variables using the data obtained by FEM. The obtained meta-model is finally used in a Pareto-based optimization approach to find the best possible combination of energy absorption, weight of structure and peak crushing force known as the Pareto fronts. The corresponding variations of geometrical design variables, known as Pareto set, constitute some important and informative design principles which can be effectively used for optimal design of aluminum foam-filled tubes.

2. Finite element analysis of crushing behavior of aluminum foam-filled tubes

In this section, finite element simulation is performed in accordance with one of the test experiments carried out by Seitzberger et al. [22]. The specimen has 4 cm outer width, 25 cm length and its wall thickness is 1.5mm. Steel tubes have been made of RSt37 and obtained from electrically welded precision profiles. Uniaxial tension test results of material are shown in Figure 1. The tube was filled with aluminum foam (base material AlMg0.6Si0.3) that was produced by a powder metallurgical production method, using titanium hydride as foaming agent [9], [23]. Density of the foam is about 680 kg/m3 and its axial compression behavior is shown in Figure 2. The specimen was foamed directly using the tubes as moulds and during this foaming process the tubes were heated beyond 600C.A universal test machine was used to do experiments. To perform quasi-static test conditions and reduce influence of inertia effects, the specimen compressed without any bound between two strong steel plates with 1 mm/s loading velocity.
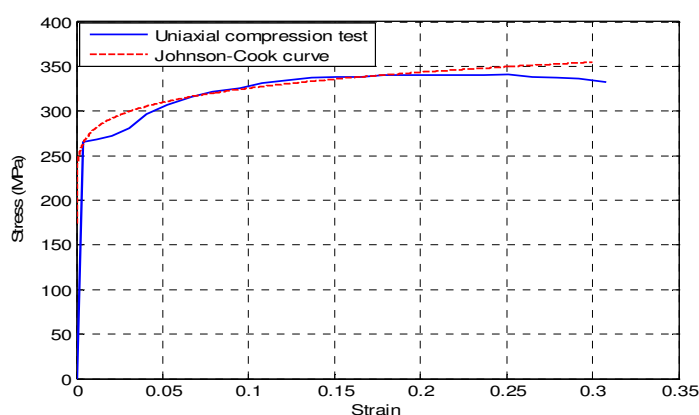

Fig1. Fitted curve of the Johnson-Cook equation on the tension test results of tube material [22].

Explicit finite element method has proven valuable in solving quasi-static problems. However, it should be noted that the explicit solution method is

developed to model the events in which inertia plays a dominant role in the solution such as high speed dynamic impact problems. Moreover, the loading rate

applied in actual quasi-static experiments is too slow which increases the time step too much. Therefore, to perform an accurate, low-cost and reliable quasi-static analysis, the inertia effects and the time step must be reduced, simultaneously. There are two special approaches which could be employed in combination to perform accurate and economic quasi-static analyses using explicit procedure.

The minimum stable time increment in the explicit dynamic analysis can be expressed as

$$\Delta t = L^e \sqrt{\frac{\rho}{E}} \qquad (1)$$

where L^e is the element length characteristic, E is the young's modulus, and ρ is the material density. According to the equation (1), artificially scaling up the material density by factor of f^2 increases the stable time increment by factor of f. Therefore, total time step will be decreased because fewer increments are required to perform the same analysis. Scaling up the mass, however, increases the inertia effects. Therefore, to ensure the quasi-static process, the loading rate should be kept very low. Another mass scaling method is the scaling down the mass of the material so that the inertial forces will be minimized. When the mass is scaling down, the stable time increments are increased and the time step of analysis will also be increased. Therefore, to reduce the time step, the loading rate must be accelerated [24]. In the

Table 1. Coefficients of curve fitted Johnson-Cook equation

A	B	N	R^2	A
1.74e8	2.192e8	0.1604	0.9709	1.74e8

present study, a semi automatic mass scaling with 2.5e6 scaling factor is applied to reduce the computational costs.

Foam filled tube was considered between two rigid plates where one plate was completely fixed and the other one was moved with 15 m/s constant axial velocity up to 150mm. Surface to surface contact was considered between plate and the tube with 0.5 friction coefficient. Tie constraint was applied between foam and wall of tube. Self-contact interaction was used to prevent interpenetration between two folds during progressive plastic fold formation.

Johnson-Cook constitutive model is used for

material modeling of steel in Abaqus/Explicit. In this

way, Johnson-Cook equation's coefficients are extracted by curve fitting using data obtained from tensile test. Johnson-Cook coefficients are presented in Table 1 and its curve is superimposed with the tensile test curve in Figure 1. It should be noted that strain rate in Johnson-Cook equation was eliminated because of low speed deformation.

Data of axial compression test of aluminum foam was used in ABAQUS/Explicit to model foam properties.

A simple uniaxial compression test is sufficient to extract foam properties. The Young' modulus and Poisson's ratio for aluminum foam were 346 MPa and 0.01 respectively. The behavior of aluminum foam was considered as isotropic crushable. 37 data points extracted from experimentally obtained stress-strain curve were entered directly for plastic behavior of the foam. The ratio of yield strength in uniaxial compression to yield strength in hydrostatic tension and the plastic Poisson's ratio [25] were also 0.95 and 0 respectively. Uniform distribution density was exerted 680 kg/m3 as well.(figure 2)

Internal energy, kinetic energy and plastic dissipation energy obtained from numerical simulation are depicted in Figure 3. According to this figure, kinetic energy is very small compared to the internal energy and therefore the numerical simulation can be considered as a quasi-static analysis, confidently.

To validate numerical model by experimental results four parameters were considered; maximum peak force, total absorbed energy, mean crush force and crush force efficiency. The results of numerical simulation and experimental test are depicted in Table 2. The force-displacement diagram and structure deformation obtained numerically are compared with the results of experiment performed by Seitzberger et al. [22] in Figure 4 and Figure 5. In Figure 4 and 5, it can be observed that the number of force-displacement peaks and troughs in numerical model are similar to experimental results and also the numerical and experimental fold formations are identical. According to Table 2 and Figures 4 and 5 numerical models predicts experimental results properly and the model can be implemented for more analyses.

There are various parameters such as tube thickness (t), tube width (C) and A factor in Johnson-Cook equation of tube material that affect energy absorption and peak crushing force.
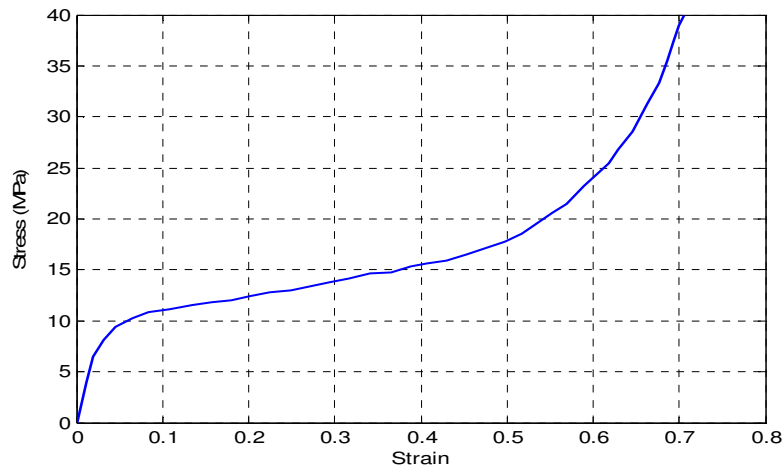
Fig2. Uniaxial compression test results of aluminum foam with 680kg/m^3 density [22].
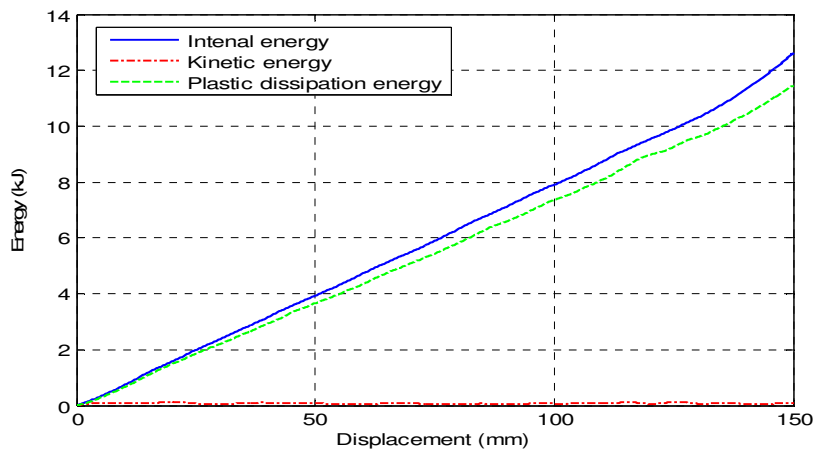

Fig3. Kinetic, internal and plastic dissipation energy for an aluminum foam-filled tube under quasi-static loading
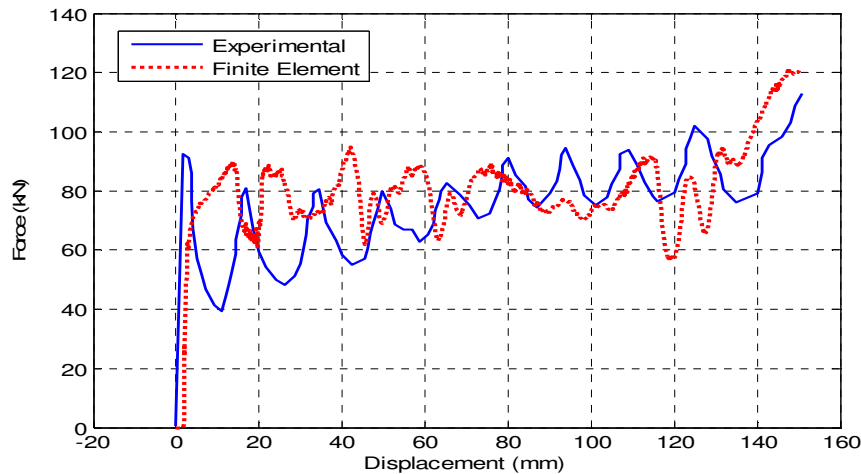

Fig4. Experimentally [22] and numerically obtained crushing force-displacement responses of aluminum foam-filled tube

Therefore, by changing the geometrical and material independent parameters t,C and A various designs will be generated and evaluated by the finite element method using ABAQUS software. Consequently, a meta-model can be constructed using the MLF neural networks, which will be further used

for multi-objective Pareto based design of such energy absorption structure. In this way, 30 various analyses is performed using non-linear ABAQUS/Explicit to simulate quasi-static test. Results for some of the models are represented in Table 3.

Fig5.. Comparison of experimental deformation [22] with numerical prediction.

3. Modeling Using Multi-layer Feed-forward Neural Networks

In principle, neural network has the power of a universal approximator, i.e. it can realize an arbitrary mapping of one vector space onto another vector space [26-27]. The main advantage of neural networks is the fact, that they are able to use some a priori unknown information hidden in data (but they are not able to extract it). Process of 'capturing' the unknown information is called 'learning of neural network' or 'training of neural network'. In mathematical formalism to learn means to adjust the weight coefficients in such a way that some conditions are fulfilled [28].

MLF neural networks, trained with a back-propagation learning algorithm, are the most popular neural networks. MLF networks are applied to a wide variety of problems [29]. A MLF neural network consists of neurons that are ordered into layers. The first layer is called the input layer, the last layer is called the output layer, and the layers between are hidden layers.

To estimate absorbed energy and peak crushing force from the finite element simulations MLF neural networks were used. This MLF networks consist of
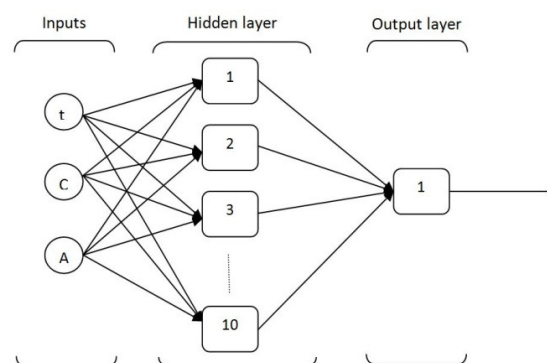

Fig6. Schematic of MLF neural networks with three layers.

one hidden layer with ten neurons and one neuron as output layer using tan-sigmoid and pulerlin transfer functions respectively. Schematic of MLF neural networks is shown in Figure 6. A back-propagation (BP) algorithm with Levenberg–Marquardt (LM) optimization technique was employed to train MLF neural networks. By reducing mean square error (MSE) for each epoch the accuracy of the networks was improved. The accuracy of neural network models are give in Tables 4, 5 and Figures 7 through 9 show comparisons between FEM results with neural network results.

The models obtained in this section are now utilized for a Pareto multi-objective crashworthiness optimization of aluminum foam-filled tubes considering the energy absorption (E), weight of structure (W), and peak crushing load (F_{max}) as conflicting objectives. Such study may unveil some interesting and important optimal design principles that would not have been obtained without the use of a multi-objective optimization approach.

4. Multi-objective crashworthiness optimization aluminum foam-filled thin-walled tube

Multi-objective optimization, which is also called multi criteria optimization or vector optimization, has been defined as finding a vector of decision variables satisfying constraints to give acceptable values to all objective functions [30-31]. In these problems, there are several objective or cost functions (a vector of objectives) to be optimized (minimized or maximized) simultaneously. These objectives often conflict with each other so that improving one of them will deteriorate another. Therefore, there is no single optimal solution as the best with respect to all the objective functions. Instead, there is a set of optimal solutions, known as Pareto optimal solutions or Pareto front [32-36] for multi-objective optimization problems. The concept of Pareto front or

set of optimal solutions in the space of objective functions in multi-objective optimization problems (MOPs) stands for a set of solutions that are non-dominated to each other but are superior to the rest of solutions in the search space. This means that it is not possible to find a single solution to be superior to all other solutions with respect to all objectives so that changing the vector of design variables in such a Pareto front consisting of these non-dominated solutions could not lead to the improvement of all objectives simultaneously. Consequently, such a change will lead to deteriorating of at least one objective. Thus, each solution of the Pareto set includes at least one objective inferior to that of another solution in that Pareto set, although both are superior to others in the rest of search space. Such problems can be mathematically defined as:

Find the vector $X^* = \left[x_1^*, x_2^*, ..., x_n^* \right]^T$ to optimize

$$F(X) = \left[f_1(X), f_2(X), ..., f_k(X) \right]^T , \quad (2)$$

subject to m inequality constraints

$$g_i(X) \leq 0 \quad , \quad i = 1 \text{ to } m , \quad (3)$$

and p equality constraints

$$h_j(X) = 0 \quad , \quad j = 1 \text{ to } p , \quad (4)$$

where $X^* \in \Re^n$ is the vector of decision or design variables, and $F(X) \in \Re^k$ is the vector of objective functions, which must each be either minimized or maximized. However, without loss of generality, it is assumed that all objective functions are to be minimized. Such multi-objective minimization

Table 2. Comparison of numerical results with experimental results [22].

	Experimental	Numerical	Error (%)
Peak Crushing Force (kN)	97	89.6	7.6
Absorbed Energy (kJ)	11.36	11.46	0.1
Mean Crush Force (kN)	75.74	76.4	0.9
Crush Force Efficiency	0.78	0.85	9

Table 3. Samples of numerical results.

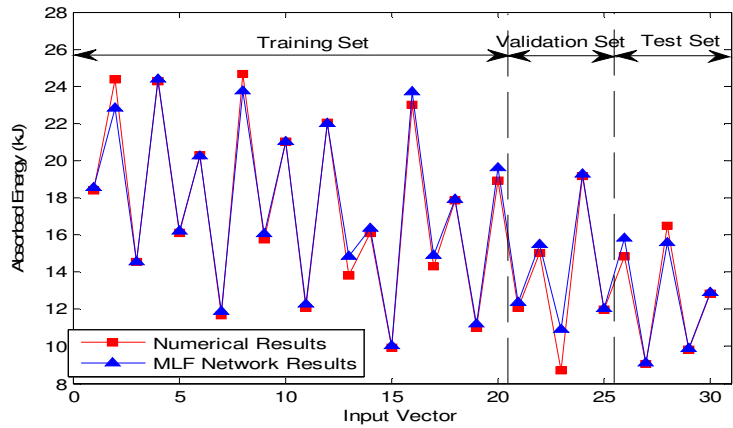| Number	t (mm)	C (mm)	A (MPa)	Absorbed Energy (kJ)	Peak Crushing Force (kN)	Weight of Structure (kg)
1	1.48	60	197	18.41	148	1.244
2	1.45	70	186	24.37	168.8	1.584
3	1.43	50	205	14.53	116.8	0.92
14	1.17	62.5	180	16.11	121.6	1.22
15	1.15	42.5	200	9.93	80	0.648
16	1.13	78.75	188	23	159.2	1.776
28	0.85	71.25	197	16.48	114.4	1.384
29	0.82	51.25	185	9.84	73.2	0.776
30	0.8	61.25	205	12.82	92	1.048

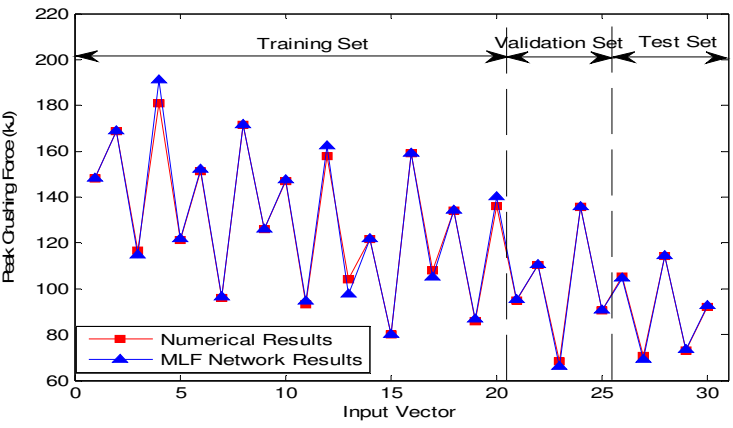**Fig7.** Variations of the absorbed energy with input data

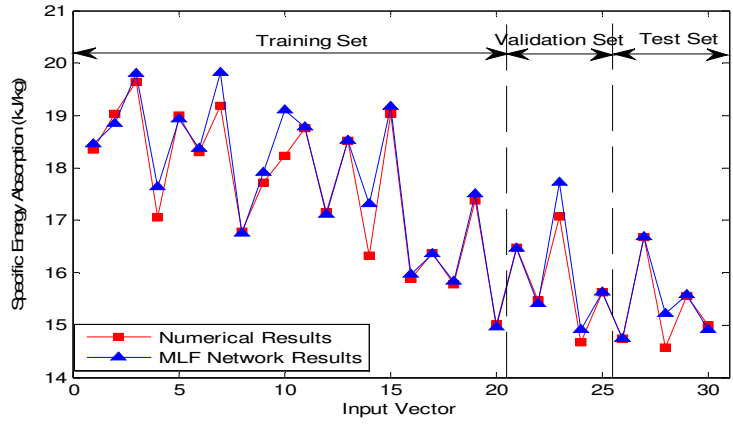**Fig8.** Variations of the peak crushing force with input data

Fig9. Variations of the specific energy absorption with input data.

Table 4. Statistical measures of the obtained MLF models for training set

	R^2	MAPE(%)	RSME
Absorbed Energy	0.993	1.517	1.9 kJ
Peak Crushing Force	0.918	0.654	11.33 kN
Specific Energy Absorption	0.973	0.764	1.265 kJ/kg

based on Pareto approach can be conducted using some definitions:

Definition of Pareto dominance

A vector $U = [u_1, u_2, ..., u_k] \in \Re^k$ is dominant to vector $V = [v_1, v_2, ..., v_k] \in \Re^k$

(denoted by $U \prec V$) if and only if quantification of the importance of each objective

Definition of a Pareto Set

For a given MOP, a Pareto set $\mathbb{P}^*$ is a set in the decision variable space consisting of all the Pareto optimal vectors

$$\mathbb{P}^* = \{X \in \Omega | \nexists X' \in \Omega : F(X') \prec F(X)\}.$$

In other words, there is no other X' as a vector of decision variables in Ω that dominates any $X \in \mathbb{P}^*$.

Definition of a Pareto front

For a given MOP, the Pareto front $\mathbb{PF}^*$ is a set of vector of objective functions which are obtained using the vectors of decision variables in the Pareto set $\mathbb{P}^*$, that is $\mathbb{PF}^*$

$$= \{F(X) = (f_1(X), f_2(X), ..., f_k(X)) : X \in \mathbb{P}^*\}.$$

In other words, the Pareto front $\mathbb{PF}^*$ is a set of the vectors of objective functions mapped from $\mathbb{P}^*$.

Evolutionary algorithms have been widely used for multi-objective optimization because of their natural properties suited for these types of problems. This is mostly because of their parallel or population-based search approach. Therefore, most of the difficulties and deficiencies within the classical methods in solving multi-objective optimization problems are eliminated. For example, there is no

$$\forall i \in \{1, 2, ..., k\}, \quad u_i \leq v_i \wedge \exists j \in \{1, 2, ..., k\} : u_j < v_j$$

In other words, there is at least one u_j which is smaller than v_j whilst the remaining u's are either smaller or equal to corresponding v's.

Definition of Pareto optimality

A point $X^* \in \Omega$ (Ω is a feasible region in $\Re^n$ satisfying equations (2) and (3) is said to be Pareto optimal (minimal) with respect to all $X \in \Omega$ if and only if $F(X^*) \prec F(X)$. Alternatively, it can be readily restated as

$$\forall i \in \{1, 2, ..., k\}, \quad \forall X \in \Omega - \{X^*\}$$

$$f_i(X^*) \leq f_i(X) \wedge \exists j \in \{1, 2, ..., k\} :$$

$$f_j(X^*) < f_j(X).$$ In other words, the solution X^* is said to be Pareto optimal (minimal) if no other solution can be found to dominate X^* using the definition of Pareto domin

need for either several runs to find the Pareto front or using numerical weights. In this way, the original non-dominated sorting procedure given by Goldberg [37] was the catalyst for several different versions of multi-objective optimization algorithms [32-33]. However, it is very important that the genetic diversity within the population be preserved sufficiently. This main issue in MOPs has been addressed by many related research works [38]. In this paper, the premature convergence of MOEAs is prevented and the solutions are directed and distributed along the true Pareto front using a recently developed algorithm, namely, the ϵ-elimination diversity algorithm by some of authors, [39].

In order to investigate the optimal design foam filled tubes in different conditions of design variables (*t, C and A*), two multi-objective (2-objective and 3-objctve) optimization problems (MOPs) have been solved. The MLF neural network models obtained in previous sections are now deployed in these 2-objective and 3-objctve optimization problems.

4.1 Two-objective optimization problem

The two conflicting objectives in this section are specific energy absorption (S*EA*) and peak crushing force (*F_max*) to be simultaneously optimized with respect to the design variables. The 2-objective optimization problem can be formulated in the following form:

$$\begin{cases} \text{Maximize} \\ f_1 = \text{SEA} \,(t,\, C,\, A) \,(\text{Specific Energy Absorption}) \\ \text{Minimize} \\ f_2 = F\,(t,\, C,\, A) \,(\text{Peak Crushing Force}) \qquad (5) \\ \\ 0.8mm < t < 1.5mm \\ 40mm < c < 80mm \\ 190MPa < A < 210MPa \end{cases}$$

Where t, C and A are thickness of the tube, width of the tube and A coefficient in the Johnson-Cook equation of tube's material respectively. The evolutionary process of Pareto multi-objective optimization is accomplished by using population size of 200 in all runs with crossover probability Pc as 0.7 for 500 generations.

Table 5. Statistical measures of the obtained MLF models for

testing set.

	R^2	MAPE (%)	RSME
Absorbed Energy	0.935	9.291	3.01 kJ
Peak Crushing Force	0.968	3.494	8.892 kN
Specific Energy Absorption	0.826	3.462	1.408 kJ/kg

The corresponding Pareto front of two objectives (SEA) and (Fmax) has been shown in Figure 10. It is clear from this figure that choosing appropriate value for specific energy absorption (SEA) or peak crushing force (Fmax), for obtaining a better value of one objective would cause a worse value of another objective. However, if the set of decision variables is selected based on each of the corresponding Pareto sets, it will lead to the best possible combination of those two objectives shown in Figure 10. In other words, if any other pair of decision variables is chosen, the corresponding values of the pair of objectives, i.e., (SEA) and (Fmax), will locate a point inferior to the obtained Pareto front. Such inferior area in the space of the two objectives is in fact up/left side of figure. Clearly, there are some important optimal design facts between the two objective functions which have been discovered by the Pareto optimization of the MLF neural network

models obtained using the finite element analysis of the aluminum foam-filled tubes. Such important design facts could not have been found without the multi-objective Pareto optimization of those MLF models. Values of peak crushing force and absorbed energy for the optimum points p, r, s and t obtained from multi-objective optimization of MLF model is presented in Table 6.

4.2 Three-objective optimization problem

A multi-objective optimization design of foam filled tube including three objectives can offer more choices for a designer. Moreover, such 3-objective optimization can subsume all those 2-objective optimization results presented in the previous section. This will allow finding trade-off optimum design points from the view point of all three objective functions simultaneously. Therefore, in this section, three objective functions, namely, energy absorption (E), weight of structure (W), and peak crushing force (F_{max}) are chosen for the multi-objective optimization. It is evident that E is maximized whilst both W and F_{max} are minimized simultaneously in a Pareto sense of the multi-objective optimization process of foam filled tubes. The 3-objective optimization problem can be formulated in the following form:

$$\begin{cases} \textit{Maximize} \\ f_1 = E\,(t,\, C,\, A)\,(\textit{Absorbed Energy}) \\ \textit{Minimize} \\ f_2 = W(t,\, C,\, A)(\textit{Weight of Structure}) \qquad (6) \\ \textit{Minimize} \\ f_3 = F_{max}\,(t,\, C,\, A)\,(\textit{Peak Crushing Load}) \\ 0.8mm < t < 1.5mm \\ 40mm < c < 80mm \\ 190MPa < A < 210MPa \end{cases}$$

A population of 400 individuals with a crossover probability of 0.7 has been used in 500 generations for such 3-objective optimization problems.

Figure 11 depicts the non-dominated individuals of 3-objective optimization in the plane of (W-E). Such non-dominated individuals of both 3-objective optimization have been shown in the plane of (W-F_{max}) and (E-F_{max}) in Figures 12 and 13, respectively. It should be noted that there is a single set of individuals as a result of the 3-objective optimization of E, W and F_{max} that are shown in different planes. Therefore, there are some points in each plane that may dominate others in the case of 3-objective optimization. However, these individuals are all non-
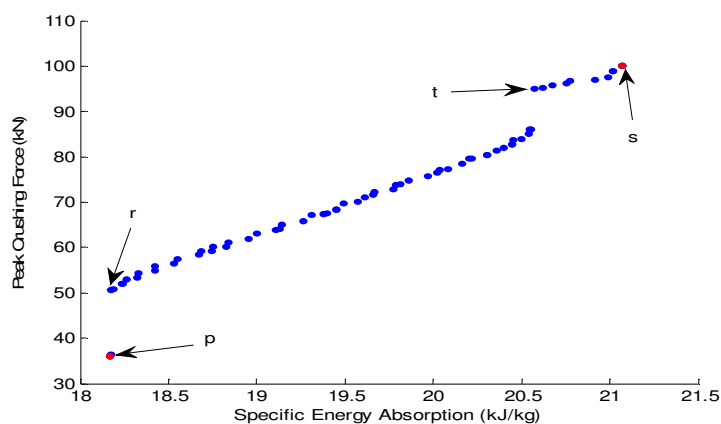
Fig10.   Pareto front of specific energy absorption and peak crushing force.

Table 6. The values of objective functions and their associated design variables of the optimum points of the 2-objective optimization

process.

Optimum Desired Points	p	r	T	s
Specific Energy Absorption (kJ/kg)	18.17	18.17	20.57	36.11
Peak Crushing Force (kN)	21.06	50.47	95.11	100.1
t (mm)	0.8	0.96	1.47	1.5
C (mm)	40	40.01	40.01	41.73
A (MPa)	190	190.06	206.51	207.11

Table 7. The values of objective functions and their associated design variables of the optimum desired points selected from the 3-objective

optimization process.

Optimum Desired Points	e	f
Absorbed Energy (kJ)	9.638	15.54
Peak Crushing Force (kN)	36.03	101.71
Weight of Structure (kg)	0.4133	0.7889
t (mm)	0.8	1.203
C (mm)	40	54.28
A (Mpa)	190	193.81

dominated when considering all three objectives simultaneously. By careful investigation of the results of 3-objective optimization it can readily be observed that the results of such 3-objective optimization provide more optimal choices for the designer.

It is now possible to seek an optimum design point (desired point) which is located almost on all Pareto fronts of Figures 11 through 13. This can be achieved by two different methods employed in this paper, namely, the nearest to ideal point method and mapping method. In the nearest to ideal point method, first, an ideal point with the best values of each objective functions is considered. Secondly, the distances among all non-dominated points to the ideal point is calculated. In this method, the desired point represents minimum distance to the ideal point. In the mapping method, the values of objective functions of all non-dominated point are mapped into interval 0 and 1. Using the sum of these values for each non-

dominated point, the desired point simply represents the minimum of the sum of those values.

Optimum design points e, f are the points which have been obtained from the nearest to ideal point method and mapping method, respectively. In the figure 12, plain of (W- F_{max}), point e dominates point f. Further, both points e and f are non-dominated as they shown in Figures 11 and 13, the plane of (W-E) and the plain of (E- F_{max}) respectively. The comparison of the values of objective functions associated with the optimum points e and f obtained from the 3-objective functions optimization is given in Table 7.

Consequently, such multi-objective optimization of energy absorption (E), weight of structure (W) and peak crushing load (F_{max}) provides more optional choices of design variables based on Pareto non-dominated points which can be selected from a trade-off point of view.
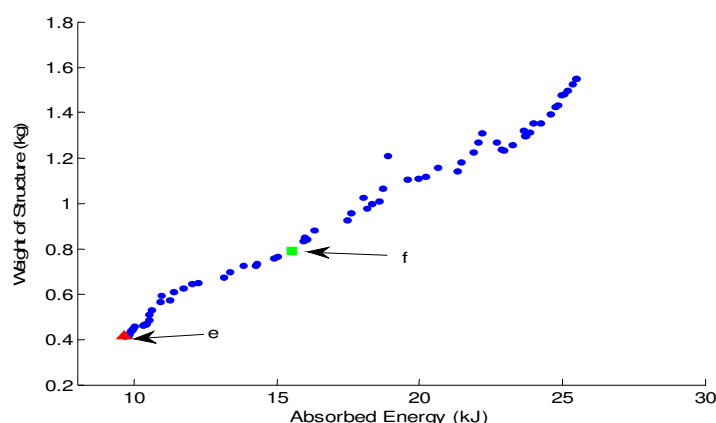

Fig11.   Absorbed energy versus the weight of structure in 3-objective optimization
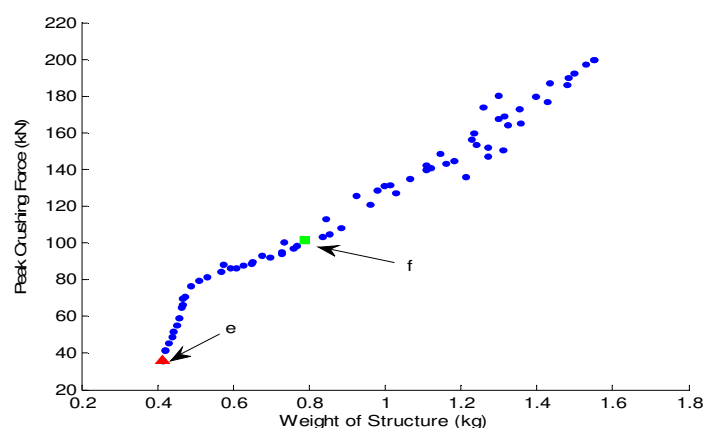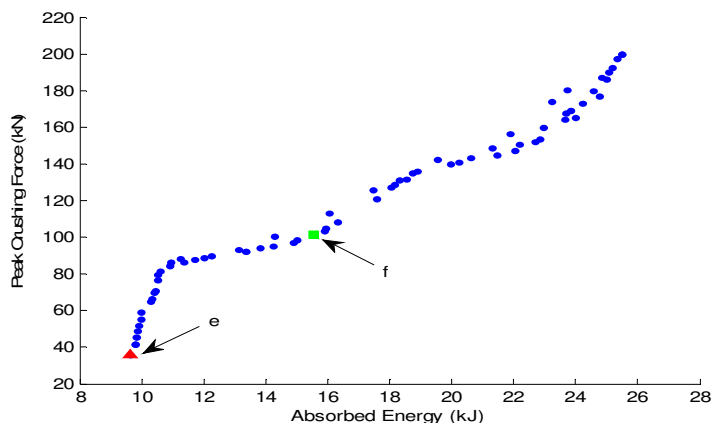
Fig12.　　Peak crushing force versus the weight of structure in 3-objective optimization

Fig13.　　Absorbed Energy versus peak crushing Force in 3-objective optimization.

5. Conclusion

Genetic algorithms have been successfully used for multi-objective Pareto based optimization of aluminum foam-filled tubes. Two different meta-model for specific energy absorption and peak crushing force have been found by multi layer feed forward neural network using some numerically obtained input-output data using the FEM. The derived meta-models have been then used in evolutionary multi-objective Pareto based optimization processes. The objective functions which conflict with each other were selected as absorbed energy (E), weight of structure (W) and peak crushing force (Fmax). The multi-objective crashworthiness optimization of aluminum foam-filled tubes led to the discovering some important trade-offs among those objective functions. Such combined application of MLF neural network modeling of numerical input-output data and subsequent non-dominated Pareto optimization process of the obtained meta-models is very promising in discovering useful and interesting design relationships.

References:

[1]. Pugsley, A.G., Macaulay, M., The large scale crumpling of thin cylindrical columns, Quart. J. Mechs and Applied Maths 13, 1960;1–9.

[2]. Johnson, W., Impact Strength of Material, London: Edward Arnold, 1972.

[3]. Jones, N., Abramowicz, W., Static and dynamic axial crushing of circular and square tubes, In: Reid SR, editor, Metal forming and Impact Mechanics. Oxford, Pergamon Press, 1985:225.

[4]. Singace, A, A. El-Sobky, H. Reddy, T. Y. On the eccentricity factor in the progressive crushing of tubes. Int J Solids Structures 32,1995, 3589–3602.

[5]. Gupta, N.K., Velmurugan, R., Consideration of internal folding and non-symmetric fold formation axisymmetric axial collapse round tubes, Int. J. Solids Structures 34, 1997, 2611–30.

[6]. Gibson, L.J., Ashby, M.F., Cellular Solids: Structure and Properties, 2nd ed. Cambridge University Press, Cambridge, New, 1997.

[7]. Gradinger, R.C., Das mechanische Verhalten von Aluminsiumschaum bei Druck- und Crushbelastung-Experimente und numerische Simulation, Diploma thesis, Vienna University of Technology, Vienna, 1997.

[8]. Gradinger, R.C., Kretz, R., Degischer, H.P., Rammerstorfer, F.G., Deformation behaviour of aluminium foam under compressive loading, In: Proceedings of JUNIOR-EUROMAT, 26±30 August 1996, Lausanne, Switzerland.

[9]. Banhart, J., MetallschaÈume, Proceedings of Symposium MetallschaÈume, 6±7 March, 1997, Bremen, Verlag MIT, Bremen.

[10]. Nariman-Zadeh, N., Darvizeh, A., Jamali, A., Pareto Optimization of Energy Absorption of Square Aluminum Columns Using Multi-

objective Genetic Algorithms, Int. J. Engineering Manufacture, Proceedings of the Institution of Mechanical Engineers, Part B, 2006, Vol 220, No.2, pp 213-224.

[11]. Astrom, K.J., Eykhoff, P., System identification, a survey, Automatica, 1971, 7-123-62

[12]. Sanchez, E., Shibata, T., Zadeh, L.A., Genetic Algorithms and Fuzzy Logic Systems, World Scientific, Riveredge, NJ, 1997.

[13]. Kristinson, K., Dumont, G., System identification and control using genetic algorithms, IEEE Trans. On Sys., Man, and Cybern, 1992, Vol. 22, No. 5, pp. 1033-1046

[14]. Koza, J., Genetic Programming, on the Programming of Computers by means of Natural Selection, MIT Press, Cambridge, MA, 1992.

[15]. Iba, H., Kuita, T., deGaris, H., Sator, T., System Identification using Structured Genetic Algorithms, Proc. Of 5th Int. Conf. On Genetic Algorithms, ICGA'93, USA, 1993.

[16]. Rodríguez-Vázquez, K., Multiobjective Evolutionary Algorithms in Non-Linear System Identification, PhD thesis, Department of Automatic Control and Systems Engineering, The University of Sheffield, Sheffield, UK, 1999.

[17]. Fonseca, C.M., Fleming, P.J, Nonlinear System Identification with Multi-objective Genetic Algorithms. Proceedings of the 13th World Congress of the International Federation of Automatic Control, 1996, 187-192, Pergamon Press, San Francisco, California.

[18]. Liu, G. P., Kadirkamanathan, V., Multiobjective criteria for neural network structure selection and identification of nonlinear systems using genetic algorithms, IEE Proceedings on Control Theory and Applications, 1999, Vol. 146, No. 5, pp. 373—382

[19]. LIPPMANN, R. P., An introduction to computing with neural nets. IEEE ASSP Magazine, 1987, 4, 4–22.

[20]. CYBENKO, G., Approximation by superposition of a sigmoidal function. Mathematics of Control, Signals, and Systems, 1989, 2, 303–314.

[21]. HORNIK, K., STINCHCOMBE, M., WHITE, H., Multilayer feedforward networks are universal approximators, Neural Networks, 1989, 2, 359–366.

[22]. Seitzberger, M., Rammerstorfer, F.G., Gradinger, R., Degischer, H.P., Blaimschein, M., Walch, C., Experimental studies on the quasi-static axial crushing of steel columns filled with aluminium foam, International Journal of Solids and Structures 37, 2000, 4125-4147.

[23]. Alulight, `Alulight material description. MEPURA, A-5282 Ranshofen, 1996.

[24]. Khalkhali, A., Masoumi, A., Darvizeh, A., Jafari, M, Shiri, A., Experimental and numericasl investigation into the quasi-static crushing behaviour of the S shape square tubes, Journal of Mechanics, December 2011, Vol. 27, No. 4.

[25]. Hassanpour, K., Ziaei-Rad, S., Finite element modeling of polypropylene foam under impact loading, In: Proceedings of the 13th annual (international) mechanical engineering conference, Isfahan University of Technology, Isfahan, Iran, May 2005.

[26]. McCulloch, W.S., Pitts, W., A logical calculus of ideas immanent in nervous activity, Bull. Math. Biophys. 5 ,1943, 115-133.

[27]. Maggiora, G.M., Elrod, D.W., Trenary, R.G., Computational neural networks as model-free mapping device, J. Chem. Inf. Comp. Sci. 32 ,1992, 732-741.

[28]. Svozil, D., KvasniEka, V., Pospichal, J., Introduction to multi-layer feed-forward neural networks, Chemometrics and Intelligent Laboratory Systems 39 ,1997, 43-62.

[29]. Zupan, J., Gasteiger,J., Neural Networks for Chemists, VCH, New York, 1993.

[30]. Coello Coello, C.A., Christiansen, A.D., Multiobjective optimization of trusses using genetic algorithms. Computers & Structures, 75, 2000, pp 647-660.

[31]. Osyezka, A., Multicriteria optimization for engineering design, in Gero, J.S., (ed.), Design Optimization, 1985, pp 193-227, Academic Press, NY

[32]. Srinivas, N., Deb, K., Multiobjective optimization Using Nondominated Sorting in Genetic Algorithms, Evolutionary Computation, 1994, Vol. 2, No. 3, pp 221-248

[33]. Fonseca, C.M., Fleming, P.J., Genetic algorithms for multi-objective optimization: Formulation, discussion and generalization. Proc. Of the Fifth Int. Conf. On genetic Algorithms, Forrest S. (Ed.), San Mateo, CA, Morgan Kaufmann, 1993, pp 416-423

[34]. Coello Coello, C.A., Christiansen, A.D., Multiobjective optimization of trusses using genetic algorithms, Computers & Structures, 75, 2000, pp 647-660

[35]. Coello Coello, C.A., Van Veldhuizen, D.A., Lamont, G.B., Evolutionary Algorithms for Solving Multi-objective problems, Kluwer Academic Publishers, NY, 2002.

[36]. Pareto, V., Cours d'economic ploitique, Lausanne, Switzerland, Rouge, 1896.

[37]. Goldberg, D. E., Genetic Algorithms in Search, Optimization, and Machine Learning. Addison-Wesley, New York, 1989.

[38]. Toffolo, A., and Benini, E., Genetic Diversity as an Objective in Multi-objective evolutionary Algorithms, Evolutionary Computation 11(2), 2003, 151-167, MIT Press

[39]. Jamali, A., Nariman-zadeh, N., Darvizeh, A., Masoumi, A., Hamrang, S., Multi-objective evolutionary optimization of polynomial neural networks for modelling and prediction of explosive cutting process, Int. J. Engineering Applications of Artificial Intelligence, In Press, Corrected Proof, Available online 20 January 2009.